Submitted to Proceedings of Pacific Ocean Remote Sensing Conference '96

Sea Ice Floe Size Distribution in the Beaufort and Chukchi Seas Measured by ERS-1 SAR

Benjamin Holt
Jet Propulsion Laboratory

Marie-Héléne Rio
Jet Propulsion Laboratory*
*On leave from Ecole National Supérieure de l'Aéronatique et de l'Espace

Abstract

This study examines the spatial and temporal character of sea ice floe size distribution during summer melt, important variables for understanding the summer heat and mass budgets and the distribution of heat between vertical and horizontal ice melt. From ERS-1 SAR imagery of the Beaufort and Chukchi Seas during 1992, an algorithm developed at the [University of Kansas was used that determines floe perimeters. The floe size distribution and fractional area of coverage have been computed. Preliminary results are presented that indicate. the gradual decrease in medium size floes (1 -5 km diameters) and a fairly steady maintenance of floes smaller than 1 km in diameter over the primary summer months within the central pack ice region. The latter result indicates that smaller floes continue to melt or decay rather than accumulate, indicating the importance of dynamics in affecting ice melt.

1. Introduction

The complete understanding of the heat and mass balance of the polar oceans includes the melting of sea ice in summer and the re-injection of fresh water back into the upper ocean. Short-wave radiation provides the heat for thinning the ice through top and bottom ablation, which is enhanced by the presence of melt ponds on the ice surface, The open water between floes also absorbs short-wave radiation, increasing lateral ice melt (Figure 1) (Maykut and Perovich, 1987). How the radiation is partitioned between vertical and horizontal melt is important since total heating of the upper ocean during summer increases as icc concentration decreases. Radiation models have shown that lateral melt is higher in areas where there arc many small (less than 200 m) floes as compared to an equivalent ice/water concentration composed only of large floes (Figure 2) (Steele, 1992). Staled another way, smaller floes melt faster than larger floes because they arc mom exposed to open water that is warmed by incoming short-wave radiation.

Sea ice melting is also affected by dynamic processes, including ice motion and the fracture of large floes into small floes by the passage of storms. While the radiation-driven melting proceeds continuous] y, the storm-driven fracturing is expected to proceed episodical y. Waves propagating into an ice cover will also breakup floes within the. ice margins. An examination of fioc size distribution by season and region may provide insight into the summer upper ocean heat budget and the relative importance of vertical and lateral melt as well as dynamic processes that affect melt.

Sea ice is a matrix of ice of various thickness and shapes, often aggregated into larger pieces by thinner ice acting as a form of Cement,]n the winter, a collection of floes may move together as rigid bodies. In the summer, the floes disintegrate and decay as the thinner ice melts away, leaving the component floes unconsolidated and isolated. As melt progresses, the isolated

larger floes become surrounded by smaller and smaller floes and chunks of ice, resulting in a sort of 'soup' or ice-water mixture.

Studies of floe size and distribution arc relatively rare, due in all likelihood to the difficulty in actually identifying qualitatively let alone quantitatively measurable floes, Rothrock and Thorndike (1984) used aerial photography and Landsat imagery on three different dates in summer to determine a floe size distribution and identified some changes in the distribution over time. Vinje (1977) used Landsat imagery to measure only those floes greater than 10 by 10 km passing through Fram Strait and found that there was a decrease in the number of all floe sizes during early summer. Hall and Rothrock (1987) measured lateral mc]t using aerial photography, finding rates as high as 10 cm per day or 1-2 m over a 20 day period, too small to measure with available satellite imagery.

Our study uses SAR imagery from the ERS-1 C-band SAR from the Beaufort and Chukchi Seas. During the summer of 1992, the satellite was in a 35-day orbital repeat cycle with about a 9 clay near-repeat cycle. The data were received and processed at the Alaska SAR Facility. Coverage extended within the station mask from the northern mask limit (Arctic central ice pack) to the icc edge in the Beaufort Sca (near Pt. Barrow) and the Chukchi Sea (cast of Wrangel island). Wc utilize an automatic algorithm dcvc.loped at the University of Kansas which effectively isolates and measures floe areas. Wc provide more detail on the data, the algorithm, analysis procedures, and preliminary results in the following sections.

2. Data Set and Characteristics of Summer Sea Ice Backscatter

Wc have utilized ERS-1 SAR C-band imagery for this study, to take advantage of the SAR's all-weather/ all -light operational capabilities and high spatial resolution, The SAR swath is 100 km wide and is obtained in strips up to 2000 km in extent. The data has an inherent resolution of about 25 m (12.5 m pixels) but wc used data that was sampled down to 225 m resolution (100 m pixels) to take advantage of the reduced size and radar speckle, despite the knowledge that we would not be able to sample floe sizes less than 100 m in area.

in the Arctic winter, ERS-1 has been found to bc particularly effective in separating the highly contrasting (bright) multiyear (MY) returns from most forms of first-year ice (darker returns) (Kwok and Cunningham, 1994; Fetterer et al., 1994). Early stages of ice growth including the periods of frost flowers on smooth thin icc and even very thick first year icc may have similar returns to MY icc (Steffen and Heinrichs, 1994). However, during and after the icc onset of melt, the contrast disappears between MY and FY ice, resulting in difficulty in distinguishing between the two major icc thickness groups due. to the wetter icc surfaces. The onset of melt is an identifiable event determined by the 4-6 dB decrease (Winebrenner et al., 1994). During summer, ablation continues and surface water drains, leaving behind melt ponds. As temperatures near freezing in the fall, the icc backscatter may vary rapidly return as air temperat urcs oscillate about freezing (Winebrenner et al., 1996). Finally, winter-like conditions prevail as the air temperatures drop well below freezing and the backscatter rapidly takes on its bright multiyear ice/ dark first-year icc contrast. Also important to consider is the effect of winds over open water leads on the radar returns. These returns arc extremely variable and may bc either brighter, similar or darker than the ice.

3. Icc Floe Algorithm

The floe algorithm is based on the so-called rest ricted growing concept, described in Soh et al. (1996), which enables separation of objects while maintaining size. The algorithm has several steps, t hc first of which separates icc from open using another technique cal led local dynamic

thresholding (Haverkamp et al., 1995). The segmentation step operates under two separate conditions, when the ice is dark and water is bright (summer) or when the ice is bright and leads/open water are dark (winter). After segmentation, the restricted growing concept is implemented, whereby objects (or floes, with definitive shape and size) are identified within the ice, followed by a shrinking process that improves identification of object separation. Next, the objects are allowed to grow back up to their size. while maintaining separation. A shape filter is then implemented which further identifies adjacent floes that appear not to be separate and have a resulting branch-like appearance. These floes are then reclassified into a class called 'discarded' floes. The portion of the ice cover that was not classified into floes are again run through a variation of dynamic thresholding so that open water and the remaining ice-water mixture are separated. Finally, the floe areas are calculated based on number of pixels,

The algorithm works best under summer conditions when the ice has dark backscatter due to surface wetness and the open water leads are radar bright from high winds. It works less well when the winds are light and when the ice is bright, due to reduced contrast. Environmental factors, especially air temperature, alter the backscatter often over very short time and space scales which creates inconsistency in the quality of the output. Often times it is extremely difficult to visually determine floe boundaries due. to uniform backscatter. Within the marginal ice zones, the variations in the ocean backscatter due to wind and currents further increases the difficulty in correct segmentation. Under these conditions, the resultant output must be inspected on an image. by image basis to select accurate results to be included in the data base. An example of high quality output is seen in Figure 3.

4. Preliminary Results and Analysis

The ERS- 1 SAR data were grouped and processed in two batches, the Beaufort data takes and the Chukchi data takes The data were then separated into time periods ('J'able 1), which were selected based on nominal environmental conditions and backscatter characteristics. From previous ERS- 1 SAR analyses of the 1992 summer Beaufort Sea ice cover, melt onset was determined to last from June 13 - June 27 (Winebrenner et al., 1994) and the onset of freeze occurred from August 27 to September 6 (Winebrenner et al., 1996). Melt and freeze proceed latitudinally so the ice cover has sharply varying (both spatially and temporally) backscatter during those periods. Periods 1 and 7 are more winter-like and the results are not satisfying during these periods. So isolating these time periods reduced the varying environmental conditions that the algorithm was working on. Next the data were binned into 2 degree latitude regions. Note that there were relatively few images above 82°N so the highest latitude bin was allowed to extend beyond the 2 degree size. This enabled comparisons of the floe data by region and time. The floe sizes were then put into 10 floe classes in terms of area ('I'able 2).

Upon analysis, we find that the variations in backscatter in response to air temperature resulted in the first two and last two periods being of marginal quality and provided no sense of any pattern in the floe size distribution. When the ice is brighter during cold temperatures, the results included are accurate but a relatively small percentage of floes of the entire ice cover are detected due to incorrect segmentation. However, during the three 20-day periods in the summer, the results were quite satisfactory. A comparison of the two regions interestingly appeared quite similar above 74°N, which is approximately the extent of the seasonal ice zone. Below this latitude, the results were variable and different in the two marginal ice zones of the Beaufort Sea near Pt. Barrow and the Chukchi Sea. This variability is not surprising since the ice pack generally remains fairly compact near Harrow and the margin of the Chukchi is adjacent to extensive open water to the south in summer, subjecting the ice to forcing from incoming waves and northward-flowing warm currents. This results in ice with different melt and ice characteristics in the two seas.

Seen in Figure 4 is a histogram showing the distribution of the fractional area covered by floes of 5 size classes, where wc combined the 6 smallest floe sizes into a single class due to the quite small percentage of floes in those classes. Focusing first on classes 2 and 3, it can be seen that the percentage of floes in these medium size classes (1 -5 km diameters) generally decreases (about 10-20%) steadily over the three time periods. Class 1 floes (less than 1 km in diameter), however, also slightly decreased over the same time rather than increased as one might expect from accumulation of continuous reduction in the medium-sized floes. This suggests that once floes made it into the smallest size range, the floes were also continuously melting away at a rate that matched accumulation. Furthermore, this also suggests the importance of dynamics on melt or the freshwater mass balance, since. small floes arc likely to be significantly assisted in their disintegration by mechanical grinding by wind and wave forcing.

The above trends and analysis do not hold in the larger floe sizes (classes 4 and 5). These classes instead increase in percentage over time. Arc medium-sized floes actually forming larger floes rather than gradually getting smaller as discussed above? This is very unlikely during the summer periods, since an accretion of floes into larger floes requires cementing together by the freezing of open water bet wccn the floes, Ocean heating cent inues throughout the summer periods and in fact more heat is absorbed as the open water leads increase in size, which serves to accelerate melt. Also there is little evidence of newly-fmcn ice in the SAR imagery, which generally shows up quite well on C-band SAR imagery (Kwok and Cunningham, 1994; Steffen and Heinrichs, 1994), Rather wc attribute the increase in the larger floe sizes to 1 or 2 possible explanations. The shape filter accounts for floes that arc too branchy and removes them from the segmented floe category. The branchy appearance or I ack of separat ion affects larger floes more than smaller floes, This problem may be seasonal, resulting in an uneven sampling for comparison. Also, there may be a decrease in area covered by floes over time, leaving large floes to account for a higher percentage of size distribution. We. are present] y anal yzing these results more carefully to resolve this question. Most likely these classes arc actually relative stable over time, since wind and wave forcing would have less impact on bigger floes,

Summary

A useful algorithm has been tested for examining the distribution of floe sizes during a summer period. Preliminary results indicate a steady decrease in floe sizes from 1-5 km diameter over time and above 74°N in the central pack ice region of the Beaufort Sea. The size of smaller floes remained fairly stable over time rather than accumulating, indicating the continuous melt of these small floes and the importance of d ynamics. 1 Difficult y in separat ing 1 arger floes (> 5 km diameter) in the early summer prevented trend analysis for these sizes. This study is the first attempt at a large-scale study of floe size changes over a summer period in the Arctic, an important measurement parameter for examining the summer heat and freshwater budgets in the polar regions.

Acknowledgments. This work was performed at the Jet l'repulsion Laboratory, California Institute of Technology under contract to the National Aeronautics and Space Administration.

References.

F. M. Fetterer, D. Gineris, and R. Kwok, "Sea Icc Type Maps from Alaska Synthetic Aperture Radar Facility Imagery: An Assessment", J Geophys. Res., 99 (C11), 22,443 -22,4S8, 1994.

R. T. Hall and D. A. Rothrock, "Photogrammetric Observations of the Lateral Melt of Sea Ice Floes", J. Geophys. Res., 92 (C7), pp. 7045-7048, 1987.

1 Iaverkamp, D., L. K. Sob, and C. Tsatsoulis, A comprehensive, automated approach to determining sea ice thickness from SAR data, IEEE Trans. Geoscience and Remote Sensing, 33, 46-57.1995.

R. Kwok and G. F. Cunningham, "Backscatter Characteristics of the Winter Icc Cover in the Beaufort Sea", J. Geophys. Res., 99 (C4), 7787-7802, 1994.

Maykut, G. A. and D. K. Perovich. The role of short-wave radiation in the summer decay of a sea icc cover, J. Geophys. Res., 92(C7), 7032-7044, 1987.

Rothrock, D. A., and A. S. Thorndike, Measuring the sca ice floe size distribution, J. Geophys. Res., 89(C4), 6477-6486, 1984.

Soh, 1..-K., D. Haverkamp, C. Tsatsoulis, and B. Holt (1996) Icc Floe Separation: The restricted growing concept and its application in floe size distribution for SAR sca ice imagery, for C. Tsatsoulis and R. Kwok (eds.), Recent Advances in the Analysis of SAR in Studies of the Polar Oceans, in preparation.

Steele, M., Sca icc melting and floe geometry in a simple icc-ocean model, J. Geophys. Res., 97(C1 1), 17,729-17,738, 1992.

K. Steffen and J. Heinrichs, "Feasibility of Sca Icc Typing with Synthetic Aperture Radar (SAR): Merging of Landsat Thematic Mapper and ERS 1 SAR Satellite Imagery", J. Geophys. Res., 99(CI 1), 22,413-22,424, 1994.

'1', E. Vinje, "Sea Icc Studies in the Spitsbergen-Greenland Area", NTIS Landsat Report li77-10206, 1977.

D. P. Winebrenner, E. D. Nelson, R. Colony, and R. D. West, "observation of Melt Onset on Multiyear Arctic Sea Icc Using the ERS 1 Synthetic Aperture Radar, J. Geophys. Res., 99 (Cl 1), 22,425-22,441, 1994.

D. P. Winebrenner, B. Holt, and E. D. Nelson, "Observations of Autumn Freeze-up in the Beaufort and Chukchi Seas Using the 1 ERS1 Synthetic Aperture Radar, J. Geophys. Res., 101(C7), 16,401-16,419, 1996.

Figure Captions

Figure 1. Ice-ocean model showing heat fluxes F and salt fluxes S during summer melt. The heat (salt) flux is positive (negative) in the direction of the arrows. After Steele (1992) and Maykut andPcrovich(1987).

Figure 2. Ocean heat and salt budgets during summer melt for initial floe diameter of 30 m (left column) and 300 m (right column). After Steele (1992).

Figure 3. A) IRS-1 SAR image from June 18, 1996, 76.2°N, 160.5°W; B) Image of algorithm output showing floe size distribution; C) floe size histogram with percentage of fractional area shown for each of 10 floe size classes.

1 igure 4. Fractional area of floe sizes during three summer time periods in the Beaufort and Chukchi Seas during 1992, separated into latitude bins. N = number of images included in the measurements. B = number of images analyzed but excluded from measurements duc to problematic output. See text for analysis.

Table 1. Selected Time Periods for 1992 Study

l'cried	Days of Year	Dates
1. Pre-melt	150-164	5/29-6/12
2. Melt Onset	165-179	6/13-6/2'7
3.Summer A	180-199	6/28-7/17
4. Summer B	200-219	7/1 8-8/06
5. summer C	220-239	8/07-8/26
6. Freeze-up onset	240-250	8/27-9/06
7. Post freeze-up	251-270	9/07-9/26

Table 2. Area and Diameter of Floe Size Classes

Class	Area (km^2)	D* (m)
1	0.01-0.64	123 - 985
2	0.64-2.56	985 - 1969
3	2.56 -16.0	1969 - 4924
4	16,0 -64.0	4924 - 9847
5	>64.0	>9847

*From Rothrock and Thorndike (1984), diameter D is related to Area A by $A = a D^2$ where a = 0.66.

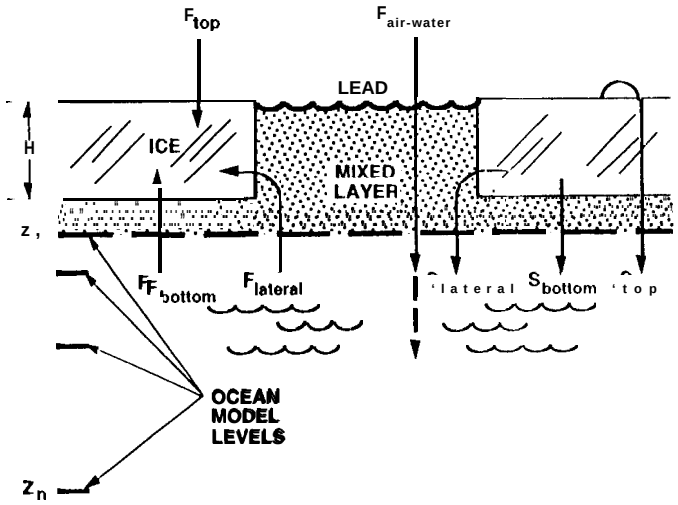

Figure 1.

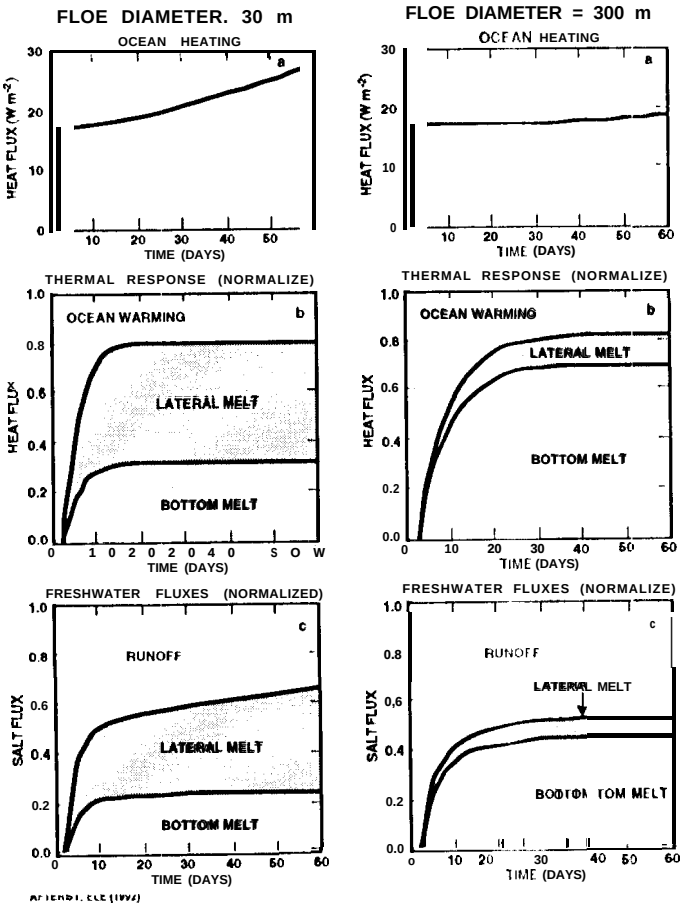

Figure 2.

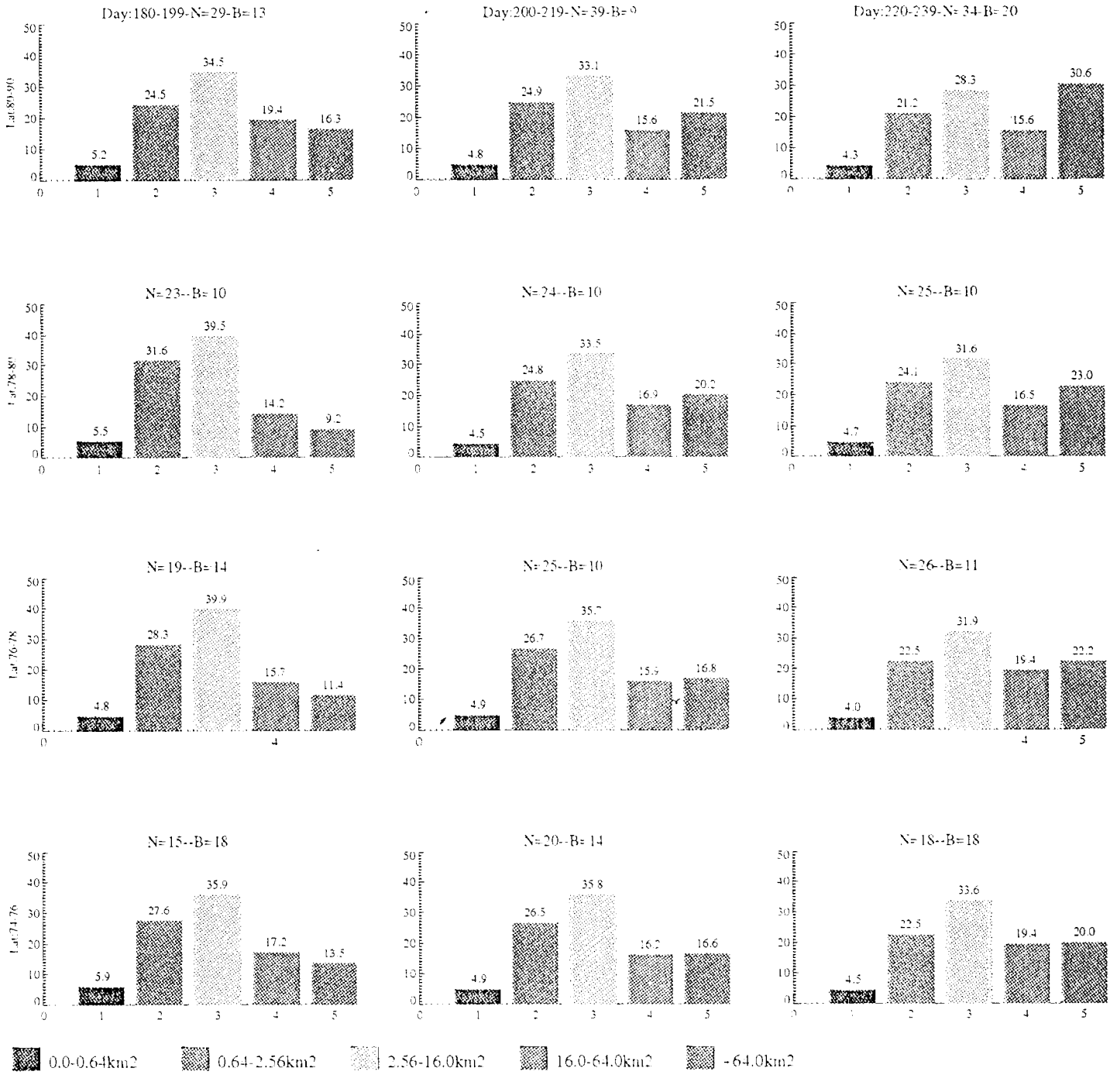
Day:180-199-N=29-B=13
5.2
24.5
34.5
19.4
16.3
Day:200-219-N=39-B=9
4.8
24.9
33.1
15.6
21.5
Day:220-239-N=34-B=20
4.3
21.2
28.3
15.6
30.6
N=23--B=10
5.5
31.6
39.5
14.2
9.2
N=24--B=10
4.5
24.8
33.5
16.9
20.2
N=25--B=10
4.7
24.1
31.6
16.5
23.0
N=19--B=14
4.8
28.3
39.9
15.7
11.4
N=25--B=10
4.9
26.7
35.7
15.9
16.8
N=26--B=11
4.0
22.5
31.9
19.4
22.2
N=15--B=18
5.9
27.6
35.9
17.2
13.5
N=20--B=14
4.9
26.5
35.8
16.2
16.6
N=18--B=18
4.5
22.5
33.6
19.4
20.0
0.0-0.64km2
0.64-2.56km2
2.56-16.0km2
16.0-64.0km2
-64.0km2

June 18

ERS-1 SAR

Floe Size

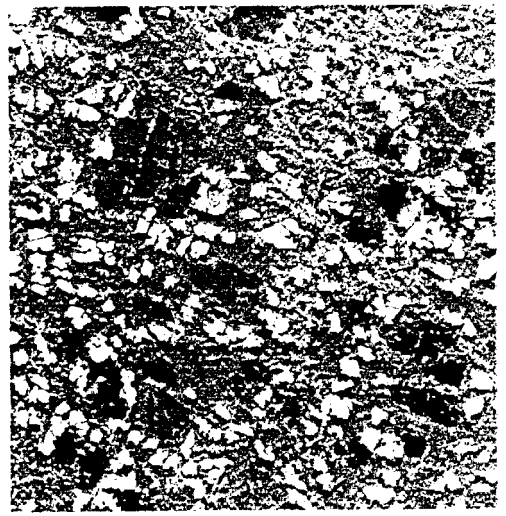

Floe Size Histogram